Detonation simulations

i. Equations
ii. Toward DNS
iii. WENO comparison

Aalto-yliopisto

Last one of special issue

GAFD Special issue on "Physics and Algorithms of the Pencil Code"

Convergence properties of detonation simulations

CHENGENG QIAN[a],CHENG WANG[a], JIANNAN LIU[b], AXEL BRANDENBURG[c,d,e*], NILS E. L. HAUGEN[f], and MIKHAIL A. LIBERMAN[c]

[a]State Key Laboratory of Explosion Science and Technology, Beijing Institute of Technology, Beijing, 100081, China
[b]College of Mining Engineering, Taiyuan University of Technology, Taiyuan 030024, China
[c]Nordita, KTH Royal Institute of Technology and Stockholm University, Roslagstullsbacken 23, SE-10691 Stockholm, Sweden
[d]Department of Astronomy, Stockholm University, SE-10691 Stockholm, Sweden
[e]JILA and Laboratory for Atmospheric and Space Physics, University of Colorado, Boulder, CO 80303, USA
[f]SINTEF Energy Research, 7465 Trondheim, Norway

(*August 12, 2019, Revision: 1.100*)

Equations

The set of equations for modelling combustion was implemented into the PENCIL CODE by Babkovskaia *et al.* (2011). Considering a mixture of $N_{\rm s}$ species undergoing $N_{\rm r}$ reactions, we solve the continuity equation for the total density ρ,

$$\frac{{\rm D}\ln\rho}{{\rm D}t} = -\boldsymbol{\nabla}\cdot\boldsymbol{U}, \tag{1}$$

the momentum equation for the velocity $\boldsymbol{U}$,

$$\frac{{\rm D}\boldsymbol{U}}{{\rm D}t} = -\frac{1}{\rho}\boldsymbol{\nabla}p + \frac{2}{\rho}\boldsymbol{\nabla}\cdot\boldsymbol{\tau}, \tag{2}$$

the energy equation for the temperature T,

$$c_v\frac{{\rm D}\ln T}{{\rm D}t} = \sum_k^{N_{\rm s}}\frac{{\rm D}Y_k}{{\rm D}t}\left(\frac{R}{W_k}-\frac{h_k}{T}\right) - \frac{R}{W}\nabla\cdot\boldsymbol{U} + \frac{\boldsymbol{\tau}:\boldsymbol{\nabla}\boldsymbol{U}}{\rho T} - \frac{\nabla\cdot\boldsymbol{q}}{\rho T}, \tag{3}$$

and the equation for the mass fraction of the kth species Y_k in the form

$$\rho\frac{{\rm D}Y_k}{{\rm D}t} = -\nabla\cdot\boldsymbol{J}_k + \dot{\omega}_k, \tag{4}$$

where ${\rm D}/{\rm D}t = \partial/\partial t + \boldsymbol{U}\cdot\boldsymbol{\nabla}$ is the advective derivative and $\tau_{ij} = 2\rho\nu{\sf S}_{ij} + \rho\zeta\delta_{ij}\boldsymbol{\nabla}\cdot\boldsymbol{U}$ are the components of the stress tensor with ${\sf S}_{ij} = \frac{1}{2}(\partial U_i/\partial x_j + \partial U_j/\partial x_i) - \frac{1}{3}\delta_{ij}\nabla\cdot\boldsymbol{U}$ being the components of the traceless rate-of-strain tensor, ν is the kinematic viscosity, ζ is the bulk

Equation of state

viscosity, $\dot{\omega}$ is the reaction rate and subscript k refers to species number k. The pressure is given by the equation of state,

$$p = \rho T \frac{R}{W} = \rho T R \sum_{k=1}^{N_s} \left(\frac{Y_k}{W_k} \right), \tag{5}$$

where R, W, and W_k are the universal gas constant, the mean molecular weight of the mixture, and the molecular weight of species k, respectively. The viscosity of species k is given by Coffee and Heimerl (1981) as

$$\mu_k = \frac{5}{16} \frac{\sqrt{\pi k_B T m_k}}{\pi \sigma_k^2 \Omega_k^{(2,2)*}}, \tag{6}$$

where σ_k is the Lennard-Jones collision diameter, k_B is the Boltzmann constant, m_k is the mass of the molecule, and $\Omega_k^{(2,2)*}$ is the collision integral (see Mourits and Rummens 1977).

Then, the viscosity of the mixture, $\mu = \rho\nu_{\mathrm{mix}}$, is given by (Wilke 1950)

$$\mu = \sum_{k=1}^{N_s} \left(X_k \mu_k \Big/ \sum_{j=1}^{N_s} X_j \Phi_{kj} \right). \tag{7}$$

Here, X_k is the mole fraction of species k and Φ_{kj} is given by

$$\Phi_{kj} = \frac{1}{\sqrt{8}} \left(1 + \frac{W_k}{W_j}\right)^{-1/2} \left[1 + \left(\frac{\mu_k}{\mu_j}\right)^{1/2} \left(\frac{W_j}{W_k}\right)^{1/4}\right]^2. \tag{8}$$

The heat flux $\boldsymbol{q}$ is given by

$$\boldsymbol{q} = \sum_{k=1}^{N_s} h_k \boldsymbol{J}_k - \lambda \boldsymbol{\nabla} T. \tag{9}$$

Here, $\boldsymbol{J}_k = \rho Y_k \boldsymbol{V}_k$ is the diffusive flux. Fick's law is employed to calculate the diffusion velocity $\boldsymbol{V}_k$ as (Poinsot and Veynante 2005)

$$\boldsymbol{V}_k = -\frac{D_k}{X_k} \boldsymbol{\nabla} X_k, \tag{10}$$

where the diffusion coefficient for species k is expressed as

$$D_k = \frac{1 - Y_k}{\sum_{j \neq k}^{N_s} X_j / D_{jk}}, \tag{11}$$

and the binary diffusion coefficient is given by

$$D_{jk} = \frac{3}{16} \frac{\sqrt{2\pi k_B^3 T^3 / m_{jk}}}{p\pi \sigma_{jk}^2 \Omega_{jk}^{(1,1)*}}, \tag{12}$$

where $\Omega_{jk}^{(1,1)*}$, σ_{jk}, and m_{jk} are given by Evlampiev (2007).

Reaction rates

The thermal conductivity for pure species k is expressed as

$$\lambda_k = \frac{\mu_k}{W_k} \left(f_{\text{trans}} \cdot C_{v,\text{trans}} + f_{\text{rot}} \cdot C_{v,\text{rot}} + f_{\text{vib}} \cdot C_{v,\text{vib}} \right), \tag{13}$$

and the thermal conductivity of the mixture follows an empirical law. The specific heat $c_{p,k}$ and specific enthalpy h_k of species k are calculated by using tabulated polynomials used in rocket science by the National Aeronautics and Space Administration (NASA) and are known as NASA polynomials. We use here the coefficients from Kéromnès *et al.* (2013).

The expression for the reaction rate is (Poinsot and Veynante 2005)

$$\dot{\omega}_k = W_k \sum_{s=1}^{N_r} \left(\nu''_{ks} - \nu'_{ks} \right) \left[k_{\text{f},s} \prod_{j=1}^{N_s} \left(\frac{\rho_j}{W_j} \right)^{\nu'_{js}} - k_{\text{r},s} \prod_{j=1}^{N_s} \left(\frac{\rho_j}{W_j} \right)^{\nu''_{js}} \right], \tag{14}$$

where ρ_k is the density of species k. Furthermore, ν'_{ks} and ν''_{ks} are the stoichiometric coefficients of species k of reaction s on the reactant and product sides, respectively. Furthermore, $k_{\text{f},s}$ is the forward rate of reaction s, which is given by

$$k_{\text{f},s} = B_s T^{\alpha_s} \exp(-E_s/RT), \tag{15}$$

where B_s is a pre-exponential factor, α_s is the temperature exponent, and E_s is the activation energy. These are all empirical coefficients that are given by the kinetic mechanism. The backward rate of reaction s is calculated from the forward rates through the equilibrium constant

$$k_{\text{r},s} = k_{\text{f},s} / k_{\text{c},s}, \tag{16}$$

Shock viscosity & WENO

2.2. ***Treatment of shocks in the*** PENCIL CODE ***and setup using the WENO code***

In the PENCIL CODE, the shock viscosity of von Neumann and Richtmyer (1950) is applied as a bulk viscosity,

$$\zeta = C_{\rm shock}\delta x^2\langle -\boldsymbol{\nabla}\cdot\boldsymbol{U}\rangle_+, \tag{17}$$

and is required to eliminate wiggles in the numerical solution. Here, $\langle ...\rangle_+$ denotes a running five point average over all positive arguments, corresponding to a compression.

In the WENO code, equations (1)–(4) are solved in the conservation form; see equations (5)–(9) of Wang *et al.* (2018). The chemical model for hydrogen-oxygen is the same model as that developed by Kéromnès *et al.* (2013). The one-dimensional simulations were performed using a DNS solver, which used the fifth order WENO finite difference scheme (Jiang and Shu 1996) to treat the convection terms of the governing equations and the sixth order standard central difference scheme to discretise the nonlinear diffusion terms. The time integration is the third order strong stability-preserving Runge-Kutta method (Gottlieb *et al.* 2001). The advantage of the WENO finite difference method is the capability to achieve arbitrarily high order accuracy in smooth regions while capturing sharp discontinuity.

2.3. *Setup of the problem*

We consider an unburned gas mixture under uniform initial conditions except for the aforementioned linear temperature gradient. The initial conditions at $t = 0$ are constant pressure and zero velocity of the unburned mixture. On the left boundary at $x = 0$, we assume a reflecting wall, where $U_x(x = 0, t) = 0$ and the initial temperature, $T(x = 0) = T^*$ exceeds the ignition threshold value. Thus, the initial conditions are as follows:

$$\begin{aligned} T(x,0) &= \begin{cases} T^* - (T^* - T_0)\, x/L, & 0 \le x \le L, \\ T_0 & x > L, \end{cases} \\ p(x,0) &= p_0, \\ \boldsymbol{U}(x,0) &= \mathbf{0}. \end{aligned} \tag{18}$$

According to the Zeldovich gradient mechanism, the reactions begin primarily at the temperature maximum, T^*, and then propagate along the temperature gradient due to spontaneous auto-ignition of the mixture. The velocity of the spontaneous reaction wave,

$$U_{\mathrm{sp}} = \frac{\mathrm{d}x}{\mathrm{d}\tau_{\mathrm{ind}}} = \left(\frac{\mathrm{d}\tau_{\mathrm{ind}}}{\mathrm{d}T}\right)^{-1} \left(\frac{\mathrm{d}T}{\mathrm{d}x}\right)^{-1} \tag{19}$$

depends on $\mathrm{d}\tau_{\mathrm{ind}}/\mathrm{d}T$ and the steepness of the temperature gradient. It could be larger than that of the pressure wave, if the temperature gradient is sufficiently shallow. Then, the coupling between the spontaneous reaction wave with the shock wave, along with the coherent energy release in the reaction, may cause shock wave amplification and the transition into a detonation wave. Since we only consider the process of detonation initiation, the parameters

Increasing resolution

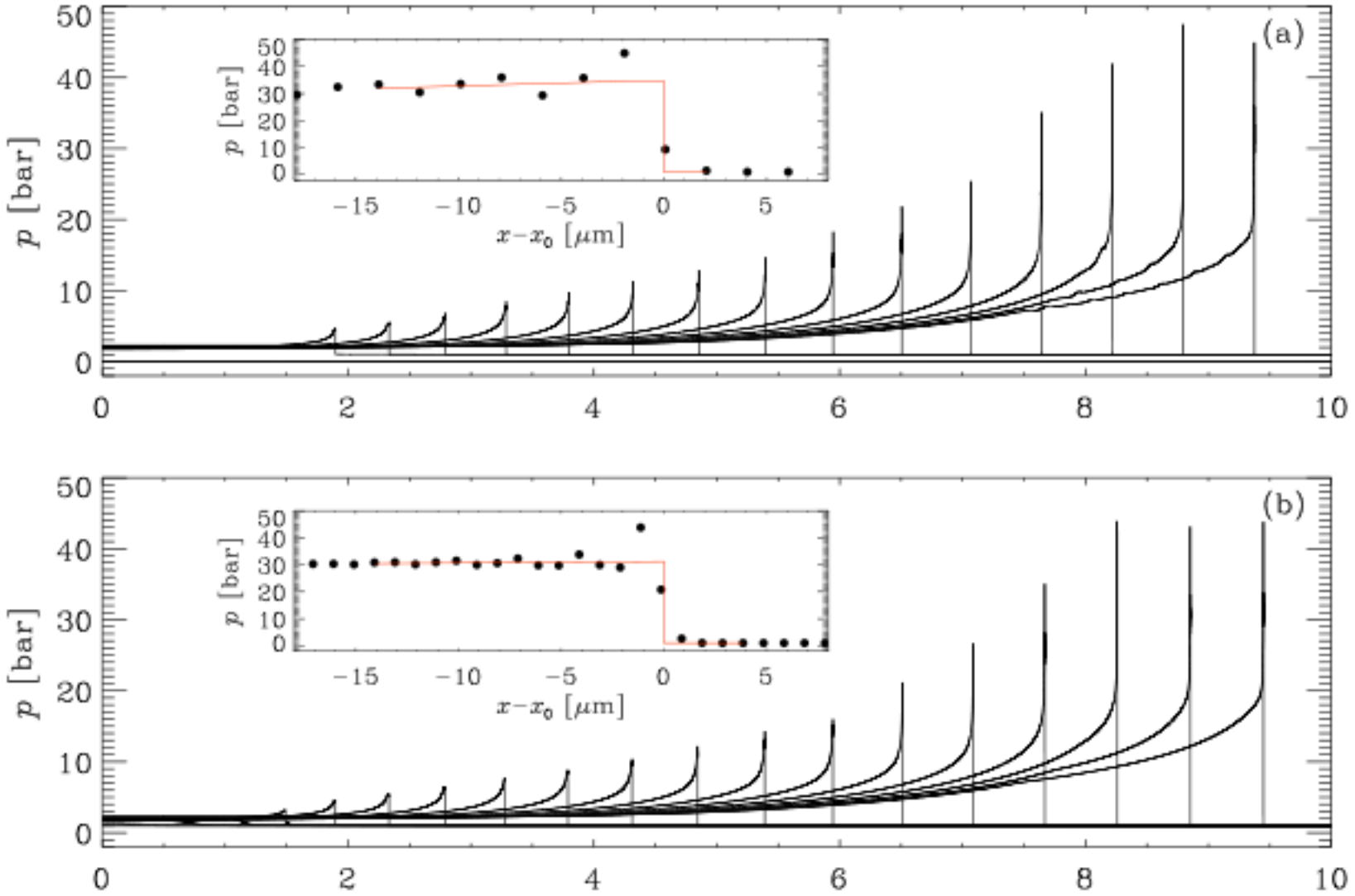

Increasing it further

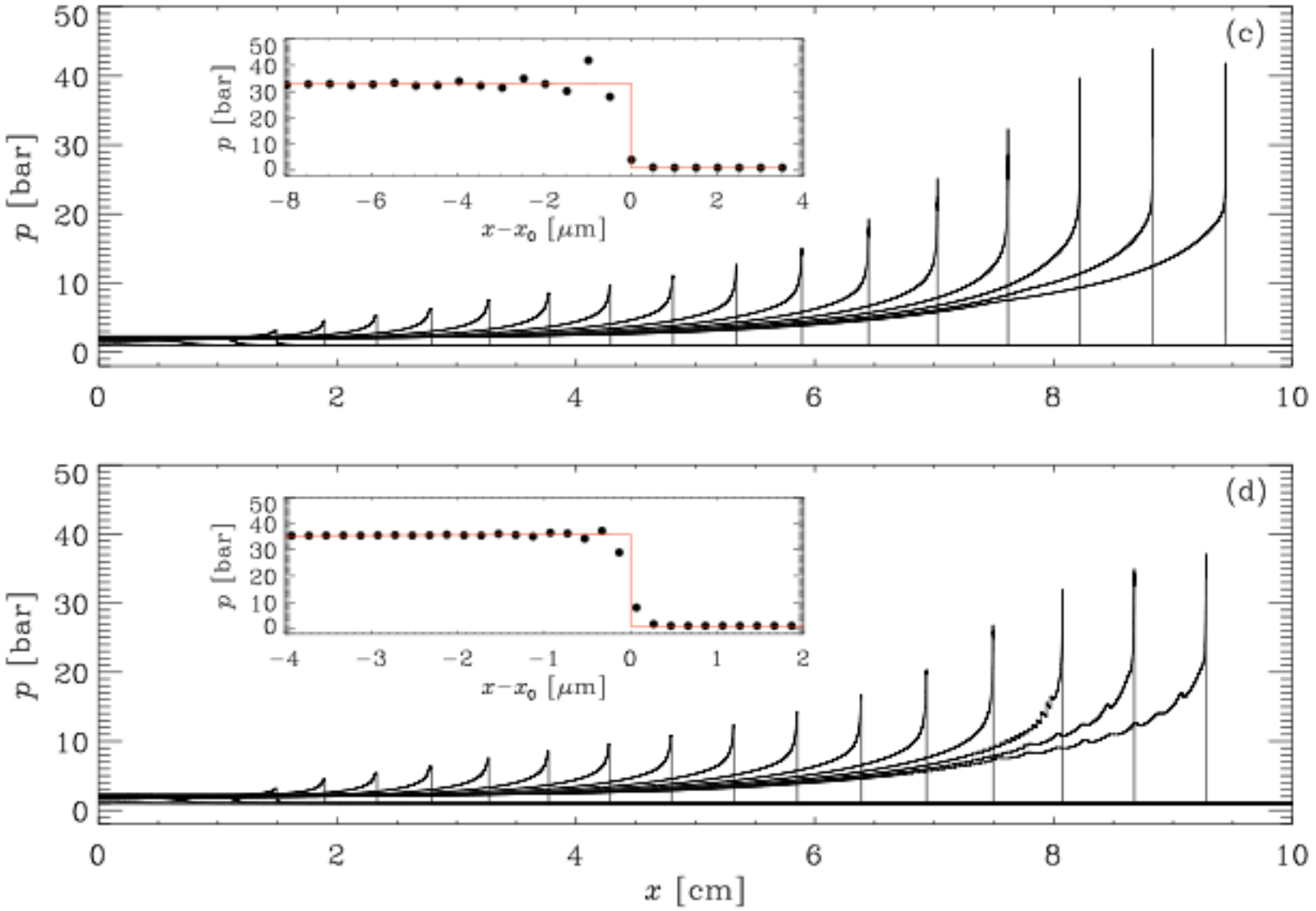

Measuring convergence

Table 1. Summary of the fit parameters at $t = 42\,\mu$s; x_0 is in cm, p_0 and p_1 are in bar, p_1' is in bar $\mu\mathrm{m}^{-1}$, L_1 and L_2 are in μm, and $\delta t_{\min}$ in ps. Runs (a)–(d) have $C_{\mathrm{shock}} = 0.8$ and run (e) has $C_{\mathrm{shock}} = 0.2$.

	δx	x_0	p_1	p_1'	L_1	L_2	N_x	N_t	$\delta t_{\min}$
(a)	1.993	9.37498	35.00	0.2200	2.56	0.36	50,176	392,000	42
(b)	0.997	9.44825	31.20	0.0546	1.21	0.30	100,352	1,266,600	24
(c)	0.498	9.44390	33.21	0.0535	0.442	0.0587	200,704	2,826,300	12
(d)	0.199	9.27530	35.78	0.1128	0.1145	0.0157	501,760	14,603,000	2.5
(e)	0.199	9.46444	28.70	0.0300	0.4069	0.1719	501,760	14,255,800	2.5

in equation (18) are chosen as follows:

$$T^* = 1500\,\mathrm{K},\ T_0 = 300\,\mathrm{K},\ L = 8\ \mathrm{cm},\ p_0 = 1\ \mathrm{bar}. \tag{20}$$

This set of parameters was also used by Liberman *et al.* (2012) to produce a steady detonation wave in a stoichiometric hydrogen–oxygen mixture.

$$L_1 = \int_{x_1}^{x_2} |p(x,t_*) - p_{\mathrm{fit}}(x,t_*)|\,\mathrm{d}x/(p_0+p_1),$$

$$L_2 = \int_{x_1}^{x_2} |p(x,t_*) - p_{\mathrm{fit}}(x,t_*)|^2\,\mathrm{d}x/(p_0+p_1)^2.$$

Scaling

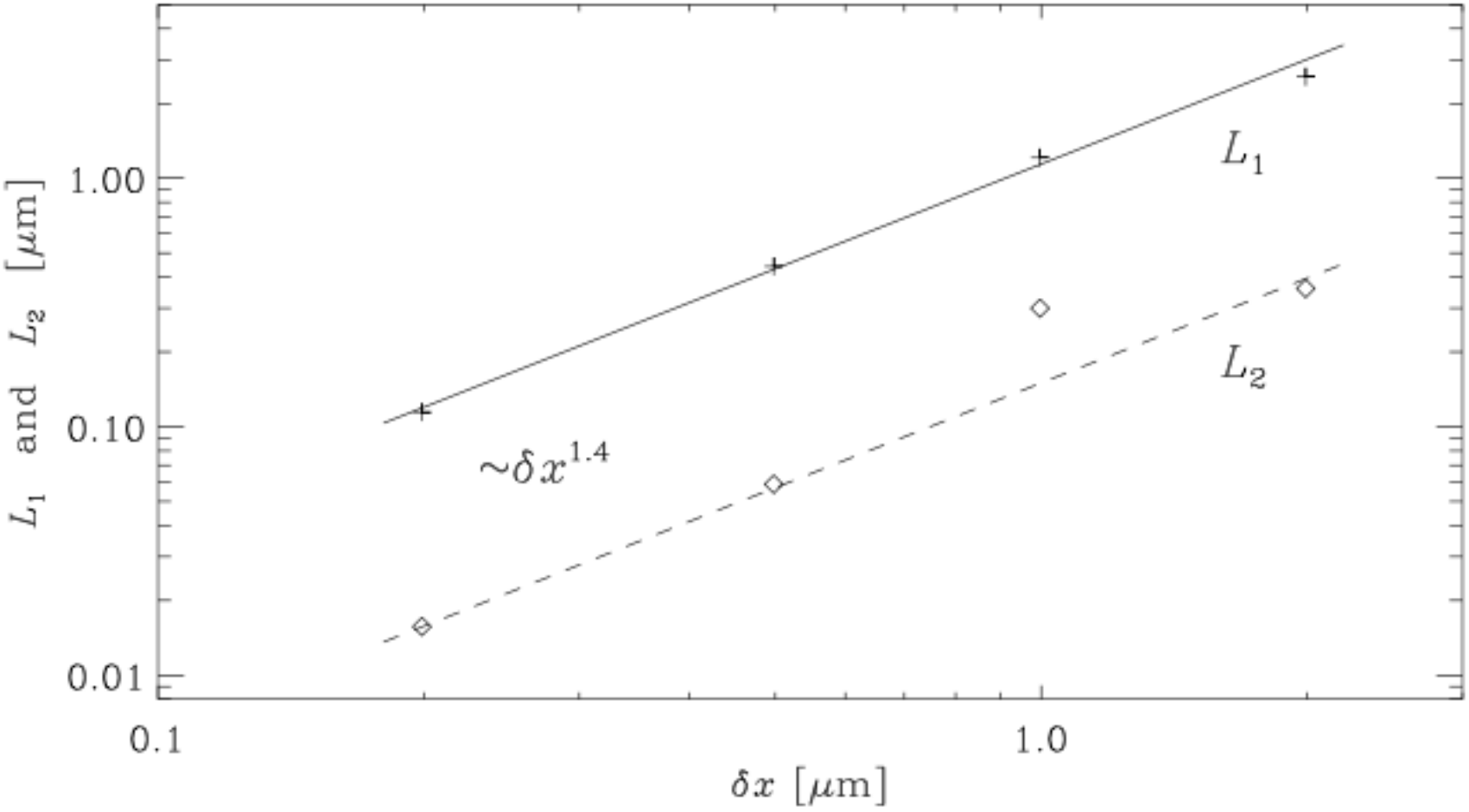

Viscosity & shock viscosity

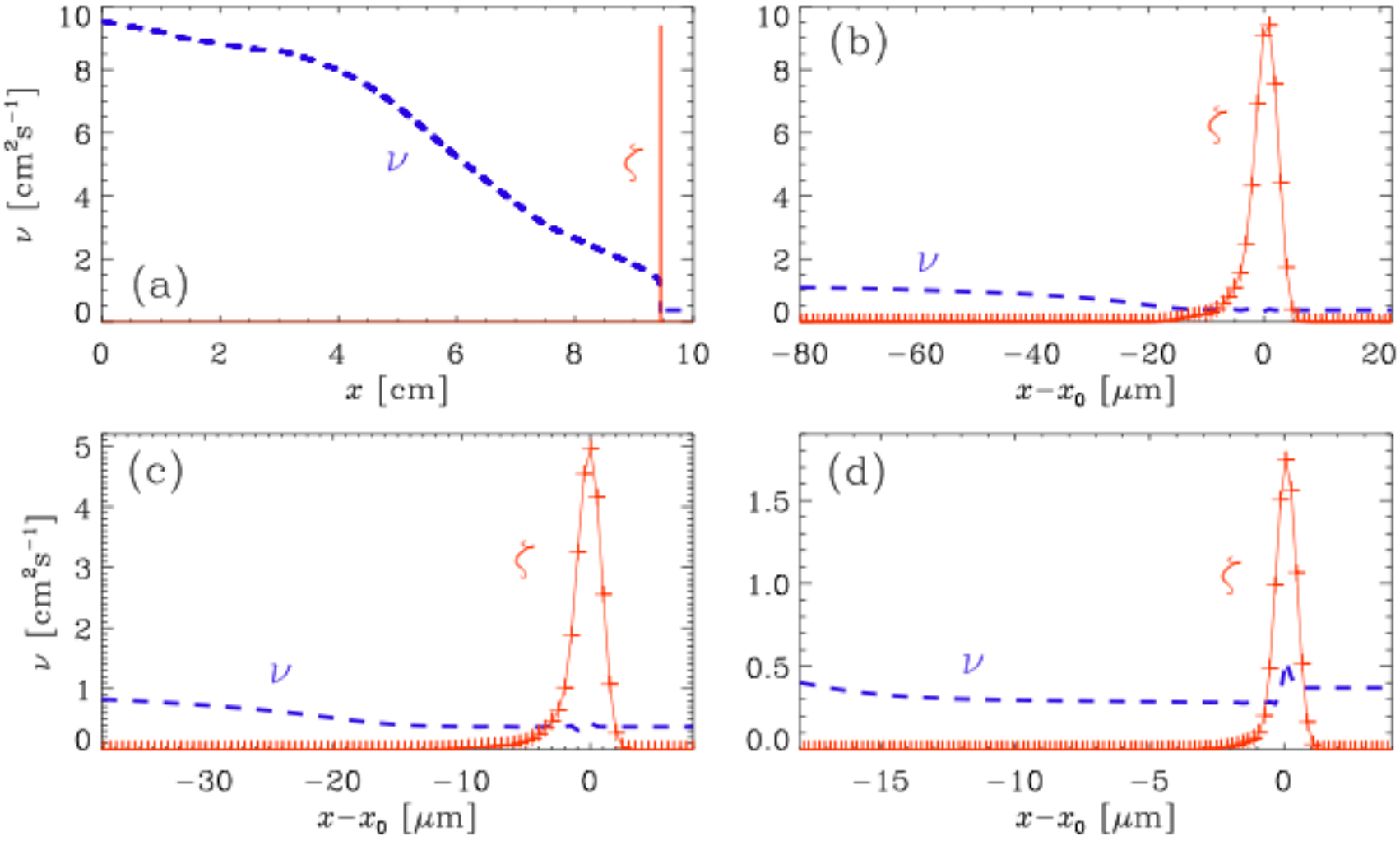

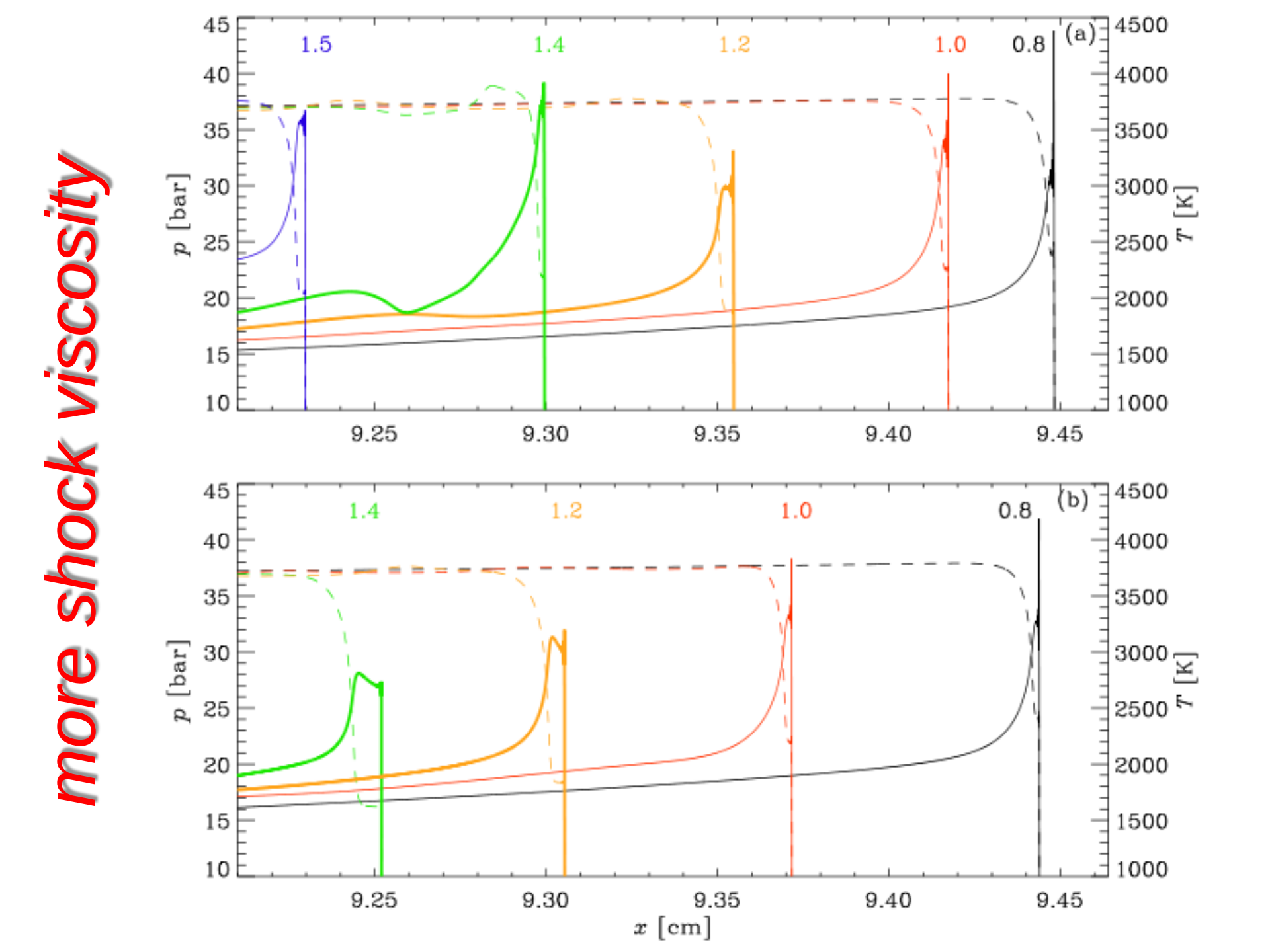
more shock viscosity
(a)
(b)
1.5
1.4
1.2
1.0
0.8
p [bar]
T [K]
x [cm]
45
40
35
30
25
20
15
10
4500
4000
3500
3000
2500
2000
1500
1000
9.25
9.30
9.35
9.40
9.45

Shock speed

$$U_\mathrm{p} = \frac{\mathrm{d}x_\mathrm{p}}{\mathrm{d}t} = -\frac{\mathrm{d}}{\mathrm{d}t}\int_0^{x_\mathrm{max}} \max(p_\mathrm{crit} - p,\, 0)/(p_\mathrm{crit} - p_0)\,\mathrm{d}x,$$

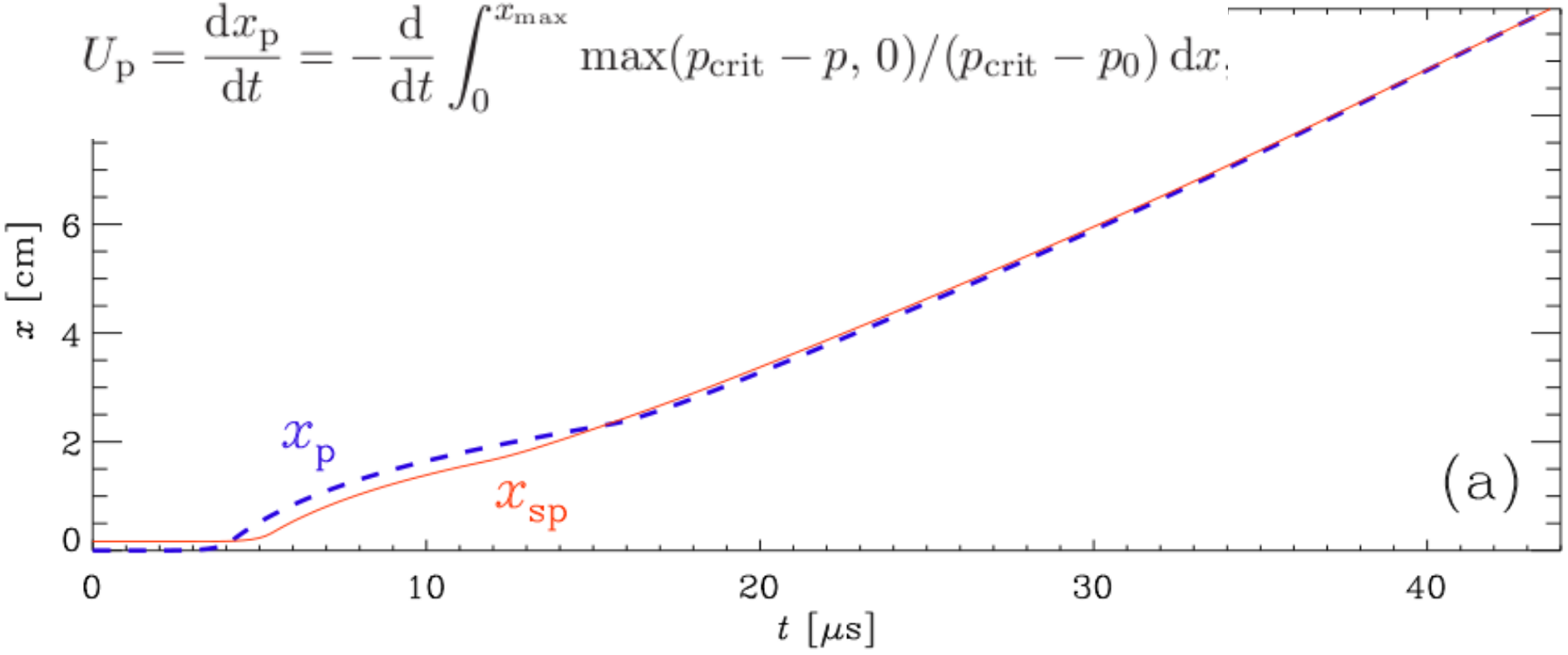

$$U_\mathrm{sp} = \frac{\mathrm{d}x_\mathrm{sp}}{\mathrm{d}t} = -\frac{\mathrm{d}}{\mathrm{d}t}\int_0^{x_\mathrm{max}} \max(1 - Y_k/Y_{k0},\, 0)\,\mathrm{d}x,$$

Front speed: derivative

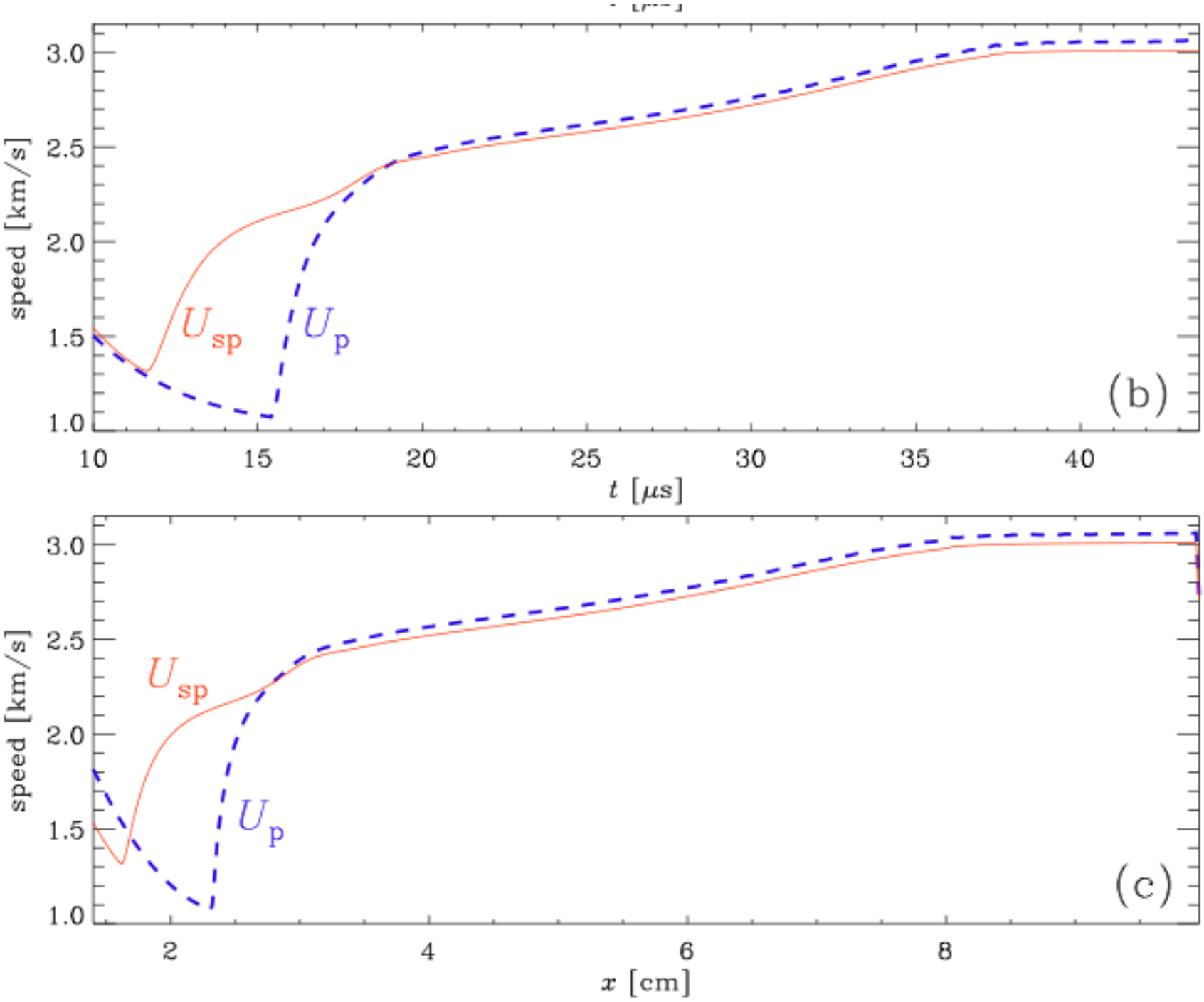

Comparison with WENO

> switching to a different spatial resolution. This, of course, suggests
> that a more advanced shock-capturing approach (e.g. WENO, as mentioned
> in the concluding section) coupled to a conservative formulation of the
> transport equations might be better suited.

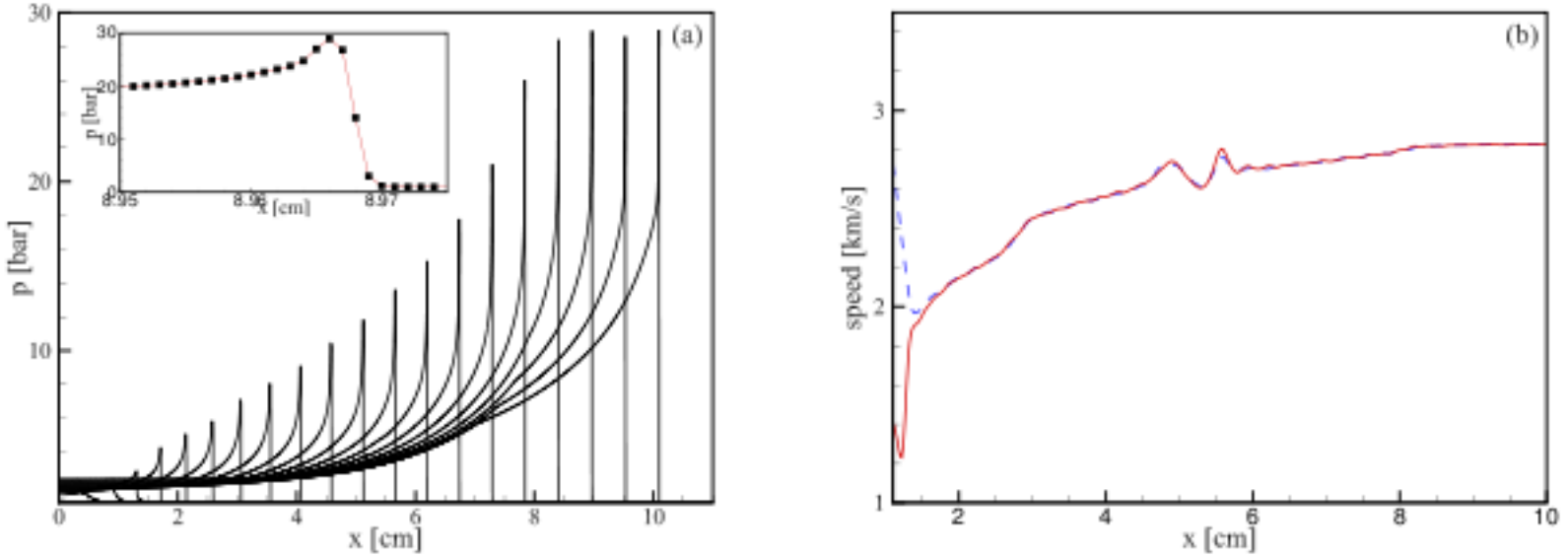

Figure 7. (a) pressure profiles calculated with the WENO code at resolution $\delta x = 10\,\mu$m, in regular time intervals from $0\,\mu$s to $46\,\mu$s. The inset shows the vicinity of the pressure peak at $42\,\mu$s. (b) corresponding spontaneous wave velocity (red solid line) and pressure wave velocity (blue dashed line).

Improved resolution

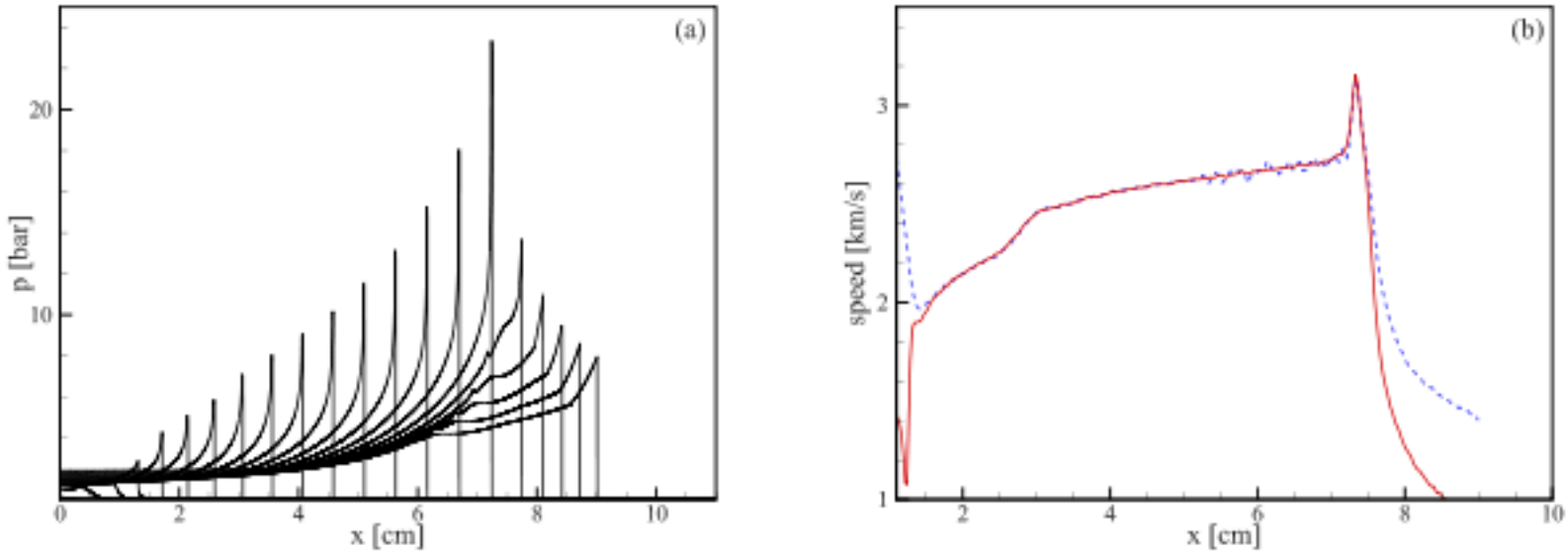

Figure 8. Similar to figure 7, but for $\delta x = 5\,\mu$m and without inset.

Decoupling of fronts

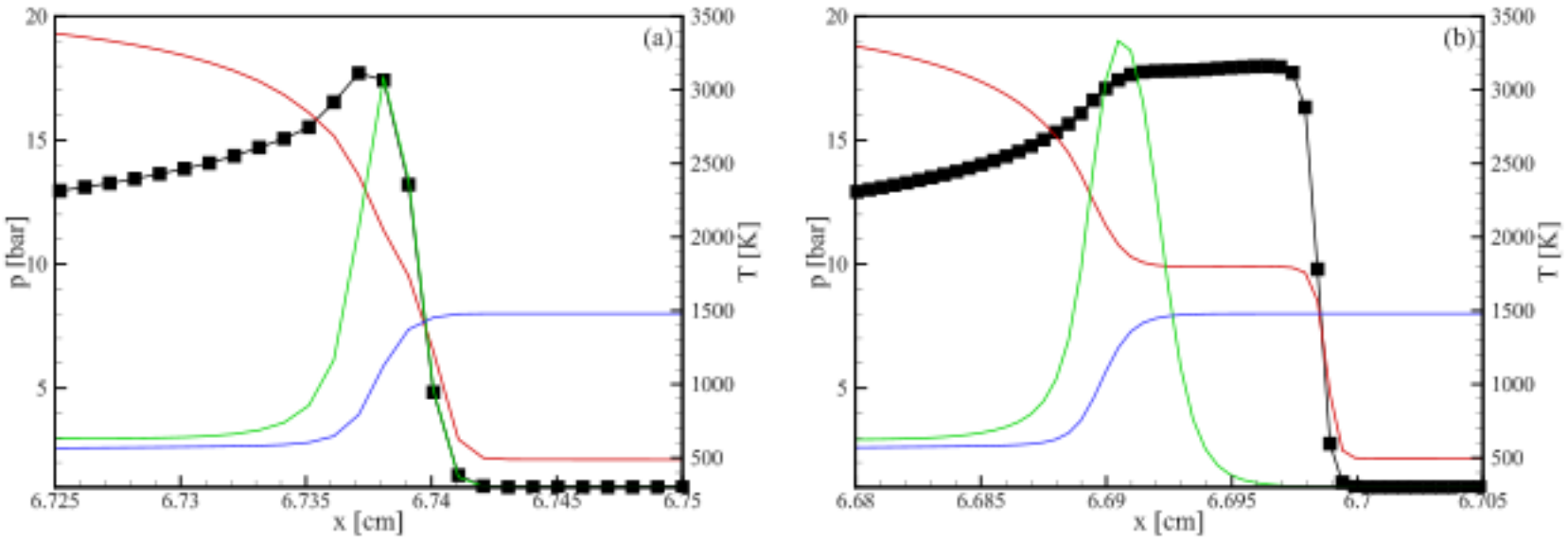

Figure 9. Profiles of pressure (black line), temperature (red line), mass fraction of HO_2 (green line), and H_2 (blue line) at $t = 34\,\mu s$, calculated with the WENO code at resolutions $\delta x = 10\mu m$ (a) and $\delta x = 5\mu m$ (b).

WENO w/ artificial viscosity

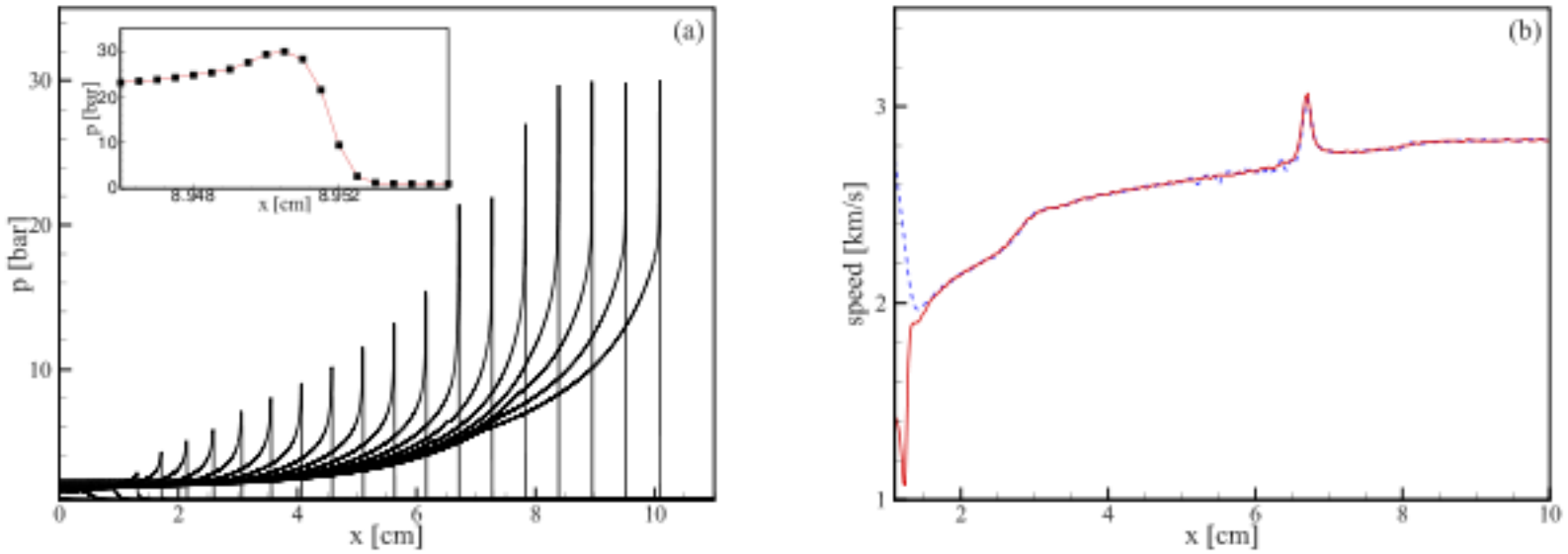

Figure 10. Similar to figure 7, but for $\delta x = 5\,\mu$m and with artificial viscosity.

Conclusions

- Convergence demponstrated w/ Pencil Code
- Should try to simulate in comoving frame to eliminate timestep constraint in hot and viscous wake
- High-order WENO without shock viscosity diverges at higher resolution